

Ion-induced disconnected branching tree morphology: correlation of fractal dimension with ion fluence

This article has been downloaded from IOPscience. Please scroll down to see the full text article.

1989 J. Phys.: Condens. Matter 1 10187

(<http://iopscience.iop.org/0953-8984/1/50/019>)

View [the table of contents for this issue](#), or go to the [journal homepage](#) for more

Download details:

IP Address: 171.66.16.96

The article was downloaded on 10/05/2010 at 21:20

Please note that [terms and conditions apply](#).

LETTER TO THE EDITOR

Ion-induced disconnected branching tree morphology: correlation of fractal dimension with ion fluence

C H Shang[†] and B X Liu^{†‡}

[†] Department of Materials Science and Engineering, Tsinghua University, Beijing 100084, People's Republic of China

[‡] Centre of Condensed Matter and Radiation Physics, CCAST (World Laboratory), Beijing, People's Republic of China

Received 10 July 1989

Abstract. We report experimental evidence of an ion-induced disconnected branching tree morphology (DBTM) as a new fractal structure. The DBTM fractal is characterised by the discontinuity of pattern components and the intrinsic branching angles. It is found that the fractal dimension of the DBTM increases with increasing ion fluence. A semi-quantitative analysis is also presented to enhance our understanding of the observed phenomenon.

Random pattern growth has been an object of considerable interest over the past few years because of its emergence in widely diverse fields [1]. Further development of theoretical endeavours and computer simulation is in serious need of a large amount of detailed experimental evidence [2]. It has also been shown that [3–8] thin solid films seem to be a favourable environment for the growth of two-dimensional random patterns. It was reported [3, 4] that fractal-like structures could be observed in sputtering-deposited NbGe₂ thin films and during the crystallisation of amorphous GeSe₂ thin films. Liu *et al* [5] also presented crystalline random pattern growth in ion-irradiated amorphous Ni–Mo films. All the above fractal patterns with a dimension of about 1.7 can be explained by models based on DLA [9, 10]. Fractal structures could also be formed in ion-implanted α -Ge/Au bilayer films [6]. Recently, several papers [7, 8] have described a new kind of dense branching morphology observed during the annealing of amorphous Al–Ge alloy films. From scrutinising the above examples of pattern formation in thin solid films, it is evident that in most cases a homogeneous and isotropic background, such as an amorphous matrix, seems to be a necessary condition for the fractal patterns to grow. Most of the above fractal patterns were composed of some polycrystalline phases, and they usually extended to a linear scale of about several (or several tens of) micrometres. One can also notice that ion irradiation, a process far from equilibrium, is a valuable means of inducing random pattern growth in thin solid films [5, 6, 11].

In this letter, we show a new fractal structure, disconnected branching tree morphology (DBTM). The new fractal was developed in AgCo films and consisted of NaCl single crystals, of which the Na and Cl atoms were recoiled into AgCo films through interfacial mixing of NaCl/AgCo bilayers by ion irradiation.

It is well known that the dynamic impact of ion irradiation is able to induce intermixing at an AgCo/NaCl interface, and subsequently recoil of the Na and Cl atoms into the AgCo layer. Moreover, there exist great differences between the heats of formation of

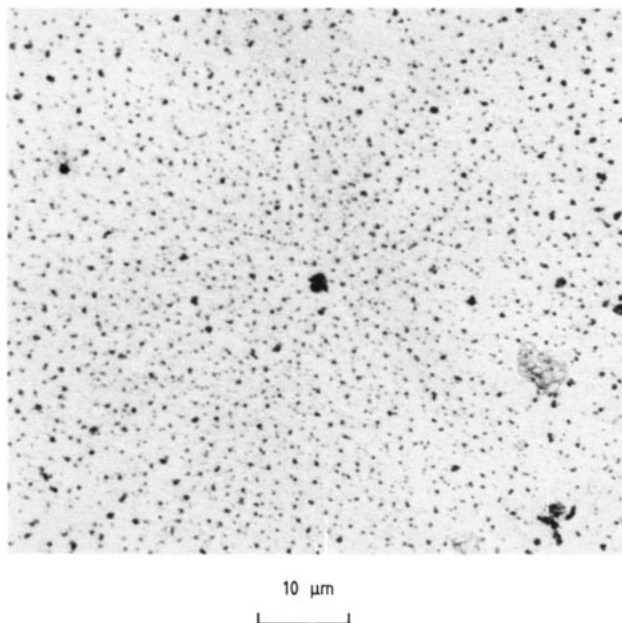


Figure 1. Bright field image of the sample irradiated with a dose of 5×10^{15} Xe ions cm^{-2} .

AgCo (+11) [12], NaCl (-411), Co_2Cl (-325.5), and AgCl (-127 kJ mol^{-1}) [13]. Obviously, Na and Cl atoms recoiled into the AgCo films by interfacial mixing will have the greatest affinity and the greatest possibility of bonding together.

Specimens were prepared by depositing alternately pure silver and pure cobalt onto cleaved NaCl single crystals at room temperature. The vacuum level during deposition was better than 2×10^{-6} Torr. There were one layer of Ag and two layers of Co, and the relative thickness was adjusted so as to have an overall composition of $\text{Ag}_{40}\text{Co}_{60}$. The total thickness of the multilayers (about 200 Å) was designed to match the depth of the maximum damage density of the incident 180 keV xenon ions. In this case, the range of the irradiation ions was about 250 Å, which meant that the ions could penetrate through the AgCo layers, resulting in mixing of Ag/Co multilayers as well as intermixing between AgCo and NaCl. The thickness of the outermost Co layer was increased by 50 Å in order to contain the sputtering effect. The as-deposited films were then irradiated with doses of 5, 10, 20, and 30×10^{15} Xe ions cm^{-2} . The target was water-cooled and the ion flux was maintained at less than 4 cm^{-2} to avoid significant heating of the specimens. The vacuum level during irradiation was better than 5×10^{-6} Torr. After ion irradiation, some Na and Cl atoms were recoiled into the AgCo films through the interface, while the remaining NaCl substrates were later dissolved in deionised water. The self-supported films were etched onto the Cu grids for transmission electron microscopy (TEM) (JEOL TEM 200CX) examination. Selected area diffraction (SAD) and *in situ* energy dispersive spectroscopy (EDS) were also used to characterise the microstructures observed in the alloy films.

TEM bright field examination showed that the as-deposited films were homogeneous in morphology and consisted of polycrystalline silver and cobalt, whereas many non-trivial patterns evolved in the Ag-Co films after ion-induced interfacial mixing. Figures 1 and 2 are two typical examples corresponding to dosages of 5 and 10×10^{15} Xi ions cm^{-2}

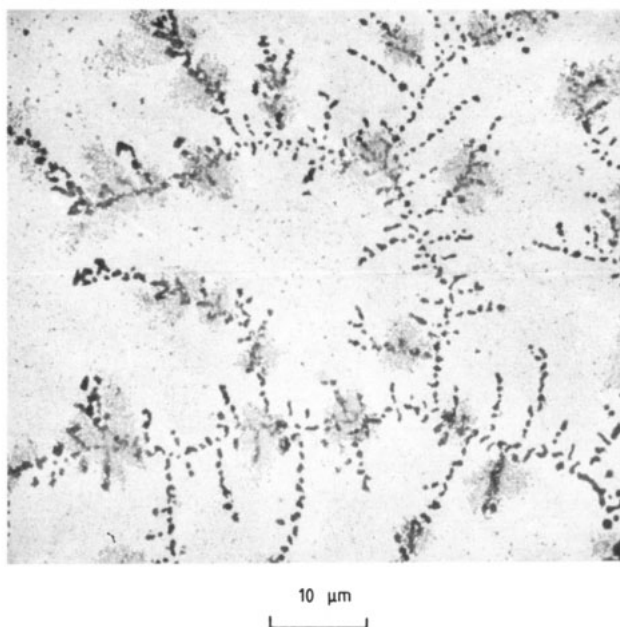


Figure 2. A typical DBTM pattern that emerged in the 1×10^{16} Xe ions cm^{-2} irradiated films.

respectively. Obviously, one conspicuous feature of this new morphology is the discontinuity of the pattern components. Each morphology with average size $100 \mu\text{m}$ is composed of $0.2\text{--}1.0 \mu\text{m}$ particles or pattern components of dark appearance. It was indicated by EDS that the dark particles were NaCl precipitates. The sharp diffraction spots of each particle further confirmed that each precipitated NaCl particle was one single crystal. The elements Na and Cl were injected into the AgCo overlayers by recoil mixing and irradiation-enhanced diffusion. The matrix is a polycrystalline mixture of Ag and Co with fine grains 200 \AA in diameter, and there was also approximately 5% Cl dissolved in the AgCo matrix as detected by EDS measurement. Another distinguishing characteristic of the self-similar DBTM patterns is the particular way in which the pattern is organised. It has been proved [14] that the form of branching is indicative of the underlying in-plane symmetry of the FCC NaCl lattice.

To examine the scale invariance of the observed structures, we have digitised the electron micrographs corresponding to the four doses with a VAX (512×512) image processor. A threshold criterion was then applied to separate the dark particles in the branches from the background. By counting the number $N(r)$ of dark pixels within the radius of gyration, r , the fractal dimension D can be obtained by following the scale law $N(r) \propto r^D$.

When the dosage was lower than 1×10^{16} Xe ions cm^{-2} (say 5×10^{15} Xe ions cm^{-2}), the fine precipitates of single NaCl crystals become homogeneously distributed in the film as shown in figure 1. This kind of morphology ($D = d = 2$) is somewhat analogous to the dense branching morphology [6, 7] except for the discontinuity of its branches. Ion irradiation at higher dosages could induce a well-organised DBTM pattern, such as that in figure 2, of which the log-log plot of $N(r)$ versus r is shown in figure 3. As listed in table 1, the fractal dimensions corresponding to doses of 1, 2, and 3×10^{16} Xe ions cm^{-2} are 1.59, 1.84, and 1.91 ± 0.05 , respectively. A measured error of 0.05 was estimated

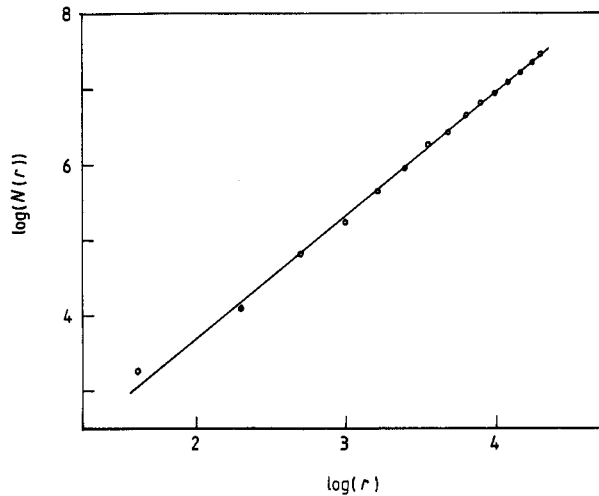


Figure 3. The log-log plot of $N(r)$ versus r corresponding to figure 2. The straight line is the least-squares fit, from which a fractal dimension of about 1.59 can be extracted.

by averaging several similar patterns observed in the same specimen. It is demonstrated that the fractal dimension of the DBTM pattern increases with the increase of the ion fluence (φ) when the dosage is higher than 1×10^{16} Xe ions cm^{-2} . Qualitatively, with the increase of ion fluence, an increasing number of Na and Cl atoms were recoiled into AgCo overlayers, resulting in the increase of the fractal dimension. A semi-quantitative analysis was further performed to give insight into the above phenomena.

Table 1. Fractal dimensions D_{obs} and D_{cal} versus ion fluence φ .

φ (10^{16} Xi ions cm^{-2})	1	2	3
D_{obs}	1.591	1.841	1.910
D_{cal}	1.585	1.843	1.907

Firstly, the fractal dimension is defined as

$$N(r) \propto r^D \quad (1)$$

where $N(r)$ is the occupied area of a fractal object within the radius of gyration r . As for the two-dimensional ($d/l = 1/100 - 1/5000$) DBTM case, it is reasonable to assume that each separate NaCl particle has the same average size or area (v), then

$$N(r) \propto v \int_0^t I(r) dt. \quad (2)$$

Here $I(r)$ is the rate of nucleation, and t is the time. When the new phase nucleates uniformly, we obtain [15]

$$I(r) \propto C\gamma \exp(-\Delta G^*/kt) \exp(-U/kt) \quad (3)$$

where C is the number of NaCl molecules per area. γ is the vibration frequency of atoms.

The nucleation energy of the critical NaCl particles is

$$\Delta G^* = -\Delta g_V V + \text{constant.} \quad (4)$$

Furthermore, Δg_V can be expressed in terms of the heat of formation ΔH_f :

$$\Delta g_V \propto \Delta H_f \quad (5)$$

and U is the activation energy of atomic migration.

From (3), (4), and (5), it follows that both ΔG^* and U take minimum values for Na and Cl combination. NaCl has therefore an overwhelmingly greater nucleation rate than any other phase. This accounts for the pattern being composed of NaCl single-crystal particles. From (1), (2), and (3), we get

$$N(r) \propto C. \quad (6)$$

Secondly, the area fraction C of NaCl particles in the films can be expected to be approximately [16]

$$C \propto 1 - \exp(-A\varphi^n). \quad (7)$$

Taking $n = 0.5^{16}$, we finally have

$$D \propto \ln(1 - \exp(-A\varphi^{1/2})). \quad (8)$$

From (8), it can be deduced naturally that an increase in φ leads to an increase in D . Applying (8) to our experimental data and using the method of recursion, we may take $A \approx 3 \times 10^{-8}$ with a fitting coefficient of 0.998. As indicated in table 1, the experimental results are in good agreement with the above semi-quantitative analysis.

In summary, we have demonstrated that a new fractal structure can be developed by intermixing at a AgCo/NaCl interface, and also that the fractal dimension increases with increasing ion fluence. This effect can be understood from our semi-quantitative analysis in terms of phase transformation theory and irradiation effects.

This study was financially supported in part by the National Natural Science Foundation of China. The authors are grateful to the staffs of the TEM Laboratories of Beijing University and the Analysis Centre of Tsinghua University for their assistance. Support from the International Atomic Energy Agency (Research Contract No 4731/RB) is also acknowledged.

References

- [1] Mandelbrot B 1982 *The Fractal Geometry of Nature* (San Francisco: Freeman)
- Matsushita M, Hayakawa Y, Sato S and Honda K 1987 *Phys. Rev. Lett.* **59** 86
- [2] Kadanoff L P 1986 *Phys. Today* **39** (2) 6
- [3] Elan W T, Wolf S A, Sprague J, Gobser D U, Van Uechter D, Barz G L Jr and Meakin P 1985 *Phys. Rev. Lett.* **54** 701
- [4] Radnoci Gy, Vicsek T, Sander L M and Grier D 1987 *Phys. Rev. A* **35** 4012
- [5] Liu B X, Huang L J, Tao K, Shang C H and Li H D 1987 *Phys. Rev. Lett.* **59** 745
- [6] Hou J G and Wu Z Q 1988 *Proc. Conf. Fractals (Shengyan, China, 1988)* p 9
- [7] Ben-Jacob E, Deutscher G, Garik P, Goldenfeld N D and Lareah Y 1987 *Phys. Rev. Lett.* **57** 1903
- [8] Deutscher G and Lareah Y 1988 *Phys. Rev. Lett.* **60** 1510
- [9] Witter T A and Sander C M 1981 *Phys. Rev. Lett.* **47** 1400; 1983 *Phys. Rev. B* **27** 5686
- [10] Meakin P 1988 *Adv. Colloid Interface Sci.* **28** 249

- [11] Shang C H and Liu B X 1989 *Nucl. Instrum. Methods* **37/38** 420
- [12] Miedema A R 1979 *Z. Metallk.* **70** 345
- [13] *Handbook of Chemistry and Physics* 1985 ed. R C Weast, 66th edn, D65 (Boca Raton, FL: CRC)
- [14] Shang C H, Liu B X and Li H D 1989 *Phys. Rev. B* at press
- [15] *Modern Crystallography III, Crystal Growth* 1984 (Berlin: Springer) and references therein
- [16] Riviere J P, Delafond J, Jaouen C, Bellara A and Dinhut J F 1984 *Appl. Phys. A* **33** 77